JBMR Plus, 2025, **9**, ziaf041
https://doi.org/10.1093/jbmrpl/ziaf041
Advance access publication: April 14, 2025
Research Article

How does bone recover in patients with tumor-induced osteomalacia? Long-term follow-up in a national cohort study

María Belén Zanchetta[1,*], Fernando Jerkovich[1,2], Florencia Scioscia[1], Yamile Mocarbel[2], Analía Pignatta[3], Natalia Elías[4], Juan Manuel Roganovich[5], Carlos Vigovich[6], María Celeste Balonga[1], Ana Carolina Cohen[7], Giselle Mumbach[8], José Luis Mansur[9], Carolina Fux Otta[10], Walter Guillermo Douthat[11], Pilar Tartaglia[12], Griselda Cecchi[13], María Bastianello[14], Luisa Plantalech[15], Erich Fradinger[1], José Rubén Zanchetta[1]

[1]IDIM, Universidad del Salvador, Instituto de DiagnÓstico e Investigaciones MetabÓlicas, Buenos Aires, C1012AAR, Argentina
[2]División Endocrinología, Hospital de Clínicas, Universidad de Buenos Aires, Buenos Aires, C1120, Argentina
[3]Servicio de Endocrinología, Servicio de Endocrinología, Hospital Interzonal San Juan Bautista, San Fernando del Valle de Catamarca, 4700, Argentina
[4]Servicio de Endocrinología, Metabolismo, Nutrición y Diabetes, Hospital Británico de Buenos Aires, Buenos Aires, C1280AEB, Argentina
[5]Clínica Ámbar, Posadas, N3300, Argentina
[6]Hospital Gobernador Centeno, General Pico, L6360, Argentina
[7]Sanatorio Rivadavia, San Miguel de Tucumán, T4000NIL, Argentina
[8]Instituto de Ortopedia y Traumatología, Posadas, N3300, Argentina.
[9]Centro de Endocrinología y Osteoporosis, La Plata, 1900, Argentina
[10]Servicio de Endocrinología, Hospital Universitario de Maternidad y Neonatología, Universidad Nacional de Córdoba, Córdoba, X500, Argentina
[11]Servicio de Endocrinología, Hospital Privado Universitario de Córdoba, Córdoba, X5016, Argentina
[12]Consultorio Privado, General Roca, R8332, Argentina
[13]Servicio de Endocrinología, Hospital Universitario Austral, Buenos Aires, B1629, Argentina
[14]Servicio de Endocrinología, Hospital Universitario CEMIC, Buenos Aires, C1406GLQ, Argentina
[15]Servicio de Endocrinología y Medicina Nuclear, Sector Osteopatías, Hospital Italiano, Buenos Aires, Buenos Aires, C1199, Argentina

*Corresponding author: María Belén Zanchetta, Libertad 836, ZC 1012 Buenos Aires, Argentina (mbzanchetta@idim.com.ar).

Abstract

Tumor-induced osteomalacia (TIO) is a rare disorder characterized by impaired bone mineralization due to phosphate wasting. Long-term changes in BMD and microarchitecture after surgical cure or medical therapy in TIO are not well understood. This study describes changes in BMD, microarchitecture, and bone strength in patients with TIO following surgical cure or medical therapy. A prospective cohort study included adults diagnosed with TIO from May 2018 to 2024, categorized into those with surgical cure and those on medical therapy. Follow-up assessments were classified as early (median 8 mo), intermediate (median 17 mo), and long-term (median 26 mo). Fifteen patients were included: seven achieved surgical cure, and eight remained on medical therapy. Lumbar spine BMD increased by +19% at early, +27% at intermediate, and +15% at long-term follow-up. Total hip BMD increased by +31%, +36%, and +31% at early, intermediate, and long-term assessments, respectively. All patients achieved a normal lumbar spine BMD, while 91% attained a normal total hip BMD. At the distal tibia, substantial increases in bone microarchitecture parameters—cortical area (Ct.Ar), cortical volumetric density (Ct.vBMD), and cortical thickness (Ct.Th)—were observed. Notably, Ct.Th improved to levels comparable to healthy controls. Bone strength improved by 13% but was not statistically significant, probably due to the small sample size. At the distal radius, most parameters remained stable. Patients with surgical cure showed more rapid and substantial improvements in BMD and cortical microarchitecture than non-cured patients, but these differences did not reach statistical significance. Overall, bone recovery in TIO is gradual, with gains in spine and hip BMD and significant improvements in tibial cortical parameters. However, some aspects of bone microarchitecture remained below control levels, underscoring the need for ongoing monitoring and individualized management strategies.

Keywords: tumor-induced bone disease, DXA, bone QCT/microCT, biochemical markers of bone turnover, PTH/Vit D/FGF23

Lay Summary

This study explores how bones recover in patients with tumor-induced osteomalacia (TIO), a rare condition that weakens bones. We followed patients who either had their tumors removed or received medical treatment over three time points, spanning from early (8 mo) to long-term (26 mo) follow-up. Our findings show that while patients who underwent surgery experienced faster bone recovery, those on medical treatment also improved over time. This research highlights the importance of continued care and monitoring to ensure bone strength returns to normal levels, helping patients with TIO regain their bone health.

Received: October 30, 2024. **Revised:** February 18, 2025. **Accepted:** February 21, 2025

Introduction

Tumor-induced osteomalacia (TIO), the most common form of acquired hypophosphatemic osteomalacia, is a rare paraneoplastic disorder driven by the overproduction of fibroblast growth factor 23 (FGF23) by a tumor.[1] Patients with TIO suffer progressively worsening musculoskeletal pain, multiple fractures, and significant functional limitations, worsened by the typically delayed diagnosis associated with rare diseases.[2] These clinical features have a catastrophic effect on patients' quality of life.[2,3]

It has been shown that patients with TIO exhibit a significant reduction in BMD at the lumbar spine, femoral neck, and total hip as measured by DXA.[3,4] Additionally, HR-pQCT has been utilized to assess bone quality in TIO patients, revealing reduced volumetric BMD (vBMD), compromised bone microstructure, and diminished bone strength at the distal radius and tibia.[5–7] These findings could likely explain why nearly 80% of these patients presented with multiple fragility fractures, with hip, vertebral, rib, and humerus fractures being the most common.[3] However, it is important to note that these methods, which rely on X-ray technology, can only assess mineralized tissue and are unable to evaluate the non-mineralized bone matrix present in osteomalacic bone.

Following resection of the tumor responsible for TIO, both serum phosphate and FGF23 levels tend to normalize rapidly.[8] Biochemical correction is often followed by gradual relief from bone pain and muscle weakness.[9] A spectacular increase of lumbar spine and hip BMD after the cure of the disease was observed by a few studies with a small number of patients and limited follow-up.[4,5,7] However, recently one study has shown that vBMD and microstructure in peripheral bone were strikingly declined in the short-term evaluation after surgical cure.[10] To date, no study has investigated long-term changes in BMD and bone microarchitecture in patients with TIO after the successful removal of the tumor or the initiation of medical therapy. Thus, it remains unclear whether bone completely recovers to its normal state in all patients following successful treatment of TIO. Does bone fully restore its structure and function after a cure? If so, how long does this process take? In cases where surgical cure is not achievable, can medical therapy alone lead to significant bone improvement?

The present study aims to provide a comprehensive assessment of bone recovery in patients with TIO by addressing several critical objectives:

1. To describe changes in BMD, bone microarchitecture, and strength observed after surgical cure or initiation of medical treatment in a group of patients with TIO. To better understand the relevance of these changes, we aim to compare the long-term microarchitectural parameters with those of a healthy control group.
2. To analyze differences in BMD and micro-architectural changes between patients who achieve surgical cure and those who do not, remaining on medical treatment.
3. As an exploratory objective, to evaluate differences in BMD and bone microarchitecture changes between patients receiving burosumab and those on conventional therapy within the non-resolved group.
4. To investigate correlations between BMD, microarchitecture changes, and biochemical parameters.

Materials and methods

Study design

A prospective cohort study is being conducted, including adult patients with a clinical diagnosis of TIO who were referred to a single bone clinic (IDIM, Universidad del Salvador), since May 2018. The study was approved by the institutional research committee (IDIM-002-2020) and by an independent ethics committee: Comité de Ética en Investigación del Instituto Nacional de Psicopatología (CEIINAPsi). This study is part of an Argentine working group conformed by trained physicians who care for patients with this condition and who have been meeting biannually since 2020 to discuss and learn about this rare disease (https://www.idim.com.ar/index.php/41-cateinvestigacionmedica/416-tio).

The protocol details have been previously described.[3,6] Briefly, during the first visit, general characteristics were gathered through medical interviews and clinical records provided by referring physicians. The main variables included were age at diagnosis, age at the onset of symptoms, gender, height, weight, duration from symptom onset to diagnosis, tumor localization, and treatment.

In the baseline and follow-up biannual visits biochemical parameters, including intact FGF-23 (iFGF-23), calcium, phosphate, creatinine, 1,25-hydroxyvitamin D, parathyroid hormone (PTH), alkaline phosphatase (ALP), and tubular reabsorption of phosphate (TRP), were assessed. Serum calcium was measured using the Cobas Integra or Cobas c Systems (Roche Diagnostics). Serum and urine phosphate and creatinine were analyzed with Beckman Coulter Synchron Systems (Beckman Coulter Inc.). PTH levels were determined using the Elecsys electrochemiluminescence assay on the Cobas e-411 platform (Roche Diagnostics). ALP was assessed with Beckman Coulter AU Chemistry Analyzers (Beckman Coulter Inc.). The 1,25-dihydroxyvitamin D concentration was measured using the Liaison XL Assay (DiaSorin Inc.). iFGF23 levels were measured using the Human intact FGF-23 ELISA Kit (Quidel-Immutopics). Additionally, DXA and HR-pQCT evaluations were performed, along with assessments of muscle mass, muscle strength, physical performance, health-related quality of life, fatigue, and pain. Renal ultrasounds, spine, hip and knee, and ankle X-rays were also included.

The diagnosis of TIO was established based on characteristic clinical features, hypophosphatemia, low tubular reabsorption of phosphate (TRP), high levels of FGF-23 or inappropriately normal for the level of hypophosphatemia, and the absence of a relevant family history. In cases without tumor localization, genetic testing to rule out other diseases as XLH was done. For tumor localization, all patients underwent a physical examination followed by 68Ga-DOTATATE-PET/CT. If suspicious lesions were identified, ultrasound, CT, or MRI was performed at the corresponding sites.

Study population

For this analysis, patients were divided into those who achieved surgical cure (resolved group) and those who did not (non-resolved group). Surgical cure was defined as: (1) sustained recovery of serum phosphate and/or FGF-23 levels and (2) the pathological confirmation of a complete phosphaturic mesenchymal tumor resection.

Inclusion criteria were having a DXA and HR-pQCT evaluation before and at least 6 mo after surgery or the start of medical treatment until June 2024. Three time points, A, B,

and C, were selected based on the availability of the highest number of data points for analysis: Time A—early follow up (median 8 mo, range 4–10 mo), Time B—intermediate follow-up (median 17 mo, range 12–21 mo), and Time C—long-term follow-up (median 26 mo, range 24–45 mo). Changes in different variables were assessed between the specific timepoints and baseline. Baseline was defined as before surgery in the resolved group or before the start of the medical treatment for the non-resolved group. Of note, some patients initiated medical treatment before surgery.

Bone mineral density

BMD was measured by DXA using GE Lunar Prodigy equipment (GE Lunar) at the lumbar spine (L1-L4) and total hip. A Z-score less than −2 was considered indicative of low BMD.

Bone microarchitecture

Bone microarchitecture of the non-dominant distal tibia and distal radius was assessed using HR-pQCT with the XtremeCT scanner (Scanco Medical AG). The scanner generates a 3D representation by acquiring 110 slices at a nominal isotropic resolution of 82 μm, focusing on 22.5 and 9.5 mm from a reference line at the endplate of the distal tibia and radius, respectively. The parameters evaluated included trabecular bone area (Tr.Ar, mm^2), cortical bone area (Ct.Ar, mm^2), trabecular density (Tb.BMD, mg HA/cm^3), cortical density (Ct.BMD, mg HA/cm^3), trabecular number (Tb.N, 1/mm), trabecular thickness (Tb.Th, mm), trabecular separation (Tb.Sp, mm), cortical thickness (Ct.Th, mm), trabecular bone volume fraction (Tb.BV/TV, %), and cortical porosity (Ct.Po, %). The method's coefficient of variation, previously published by our group, was derived from 2 consecutive measurements with complete repositioning in 56 women.[11] Reproducibility for volumetric BMD measurements ranged from 0.5% to 0.8% in premenopausal women, and from 0.4% to 3.1% for structural parameters.[11]

Healthy control subjects matched by age and sex were recruited, maintaining a 2:1 ratio of controls to patients. Potential control participants were identified among acquaintances of the research team and invited to join the study. Individuals with any bone-related conditions or those undergoing treatments that could influence bone metabolism were excluded from participation.

Bone strength

Finite element (FE) models of the radius and tibia were created from segmented HR-pQCT images using the software provided with the HR-pQCT device (IPL; Scanco Medical AG, v5.11/FE-V01.15). These linear FE models, with axial boundary conditions, were used to estimate failure load through a linear approach. Images were filtered using a Laplace–Hamming filter, and axial boundary conditions were assigned for compression tests with 1% strain (assuming a Young's modulus of 6829 MPa and a Poisson's ratio of 0.3). Failure load (kN) and total bone stiffness (kN/mm) were calculated as described in previous studies.[12]

Statistical analysis

Continuous variables with a non-normal distribution were reported as median (range), while those with a normal distribution were expressed as mean (standard deviation [SD]). Categorical data were presented as frequencies and percentages. Normality of continuous variables was assessed using the Kolmogorov–Smirnov or Shapiro–Wilk tests, as appropriate. Changes in BMD and bone microarchitecture over time were evaluated using the Friedman test for related samples (two-way analysis of variance by ranks). Significance values were adjusted using Bonferroni correction for multiple comparisons. Pairwise comparisons were performed only if the overall test result was statistically significant. For comparisons involving two samples, the Wilcoxon signed-rank test was used. Differences between independent groups were analyzed using the Mann–Whitney U test for non-normally distributed variables and the Student's *t*-test for normally distributed variables. Correlations were assessed using Spearman's test for non-parametric data and Pearson's test for parametric data. Categorical variables were compared using the chi-square test or Fisher's exact test when appropriate. Statistical analyses were conducted using IBM SPSS statistics 26.0, with a significance level set at $p < .05$. Box-and-whisker plot with individual data points was created using R software (version 4.4.2; R Core Team, 2024).

Results

Patients' general characteristics

Since 2018, 22 patients have been referred to our institution with a diagnosis or suspicion of TIO (Figure 1). Of these, 15 patients with TIO fulfilled the inclusion criteria and were included in the study: seven patients who achieved surgical cure and eight who did not. Among the non-resolved group, five patients were treated with burosumab for a median duration of 26 mo (range: 4-31), in addition to phosphate and/or calcitriol supplementation if required. General characteristics of the cohort are presented in Table 1.

Baseline clinical characteristics did not differ significantly between the resolved and non-resolved groups. Baseline biochemical data were also similar (Table 1).

Nine patients (6 resolved, 3 non-resolved) were included at time point A, with a median follow-up of 8 mo (range: 4-10). Thirteen patients (7 resolved, 6 non-resolved) were included at time point B, with a median follow-up of 17 mo (range: 12-21). Twelve patients (5 resolved, 7 non-resolved) were included at time point C, with a median follow-up of 26 mo (range: 24-45). It is important to note that, in the resolved group, two patients had received medical treatment for 63 and 82 mo prior to complete tumor resection, with one reaching normal BMD values before surgery. FE analysis was available in 6 patients (4 from the resolved group and 2 from the non-resolved group).

Throughout the entire follow-up period, only patients in the non-resolved group experienced additional fragility fractures.

Changes in BMD

At the lumbar spine, BMD increased compared to baseline, with a 19% increase at time point A, 27% at time point B, and 15% at time point C, with corresponding ranges of −5% to 67%, −3% to 125%, and −3.5% to 131%. These changes were not statistically significant (Friedman test, $p = .516$). The median lumbar spine BMD Z-score improved from −2.3 (range: −5.3 to 2.3) at baseline to −0.6 (−2.4 to 2.5) at time point A, −0.7 (−2.4 to 2.1) at time point B, and 1.3 (−2.0 to 2.6) at time point C.

At the total hip, BMD increased by 31% at time point A, by 36% at time point B and by 31% at time point C, relative to baseline, with ranges of −6% to 73%, −9% to 131%, and −9% to 155%, respectively. The overall changes are clinically relevant, even though they did not reach statistical significance

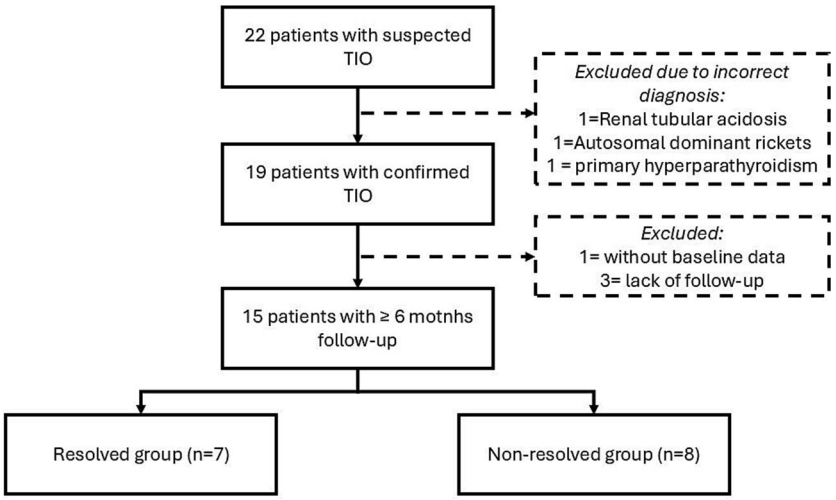

Figure 1. Flow-chart of patient selection process.

Table 1. Baseline characteristics of the cohort.

	Total ($n = 15$)	Resolved group ($n = 7$)	Non-resolved group ($n = 8$)	p
Age at diagnosis (yr)	42 ± 13.5	46 ± 7.6	37 ± 16.5	.207[a]
Age at initial symptoms (yr)	39 ± 13.6	43 ± 2.7	35 ± 16.4	.224[a]
Female sex (*n*, %)	11	4 (36)	7 (64)	.282[b]
Time to diagnosis (mo)	33 (9-95)	24 (9-95)	34 (22-49)	.463[c]
Weight (kg)	66.7 ± 22.2	66.7 ± 26.5	66.6 ± 19.6	.993[a]
Height (m)	1.51 ± 0.19	1.51 ± 0.21	1.51 ± 0.19	.990[a]
BMI (kg/m^2)	22 ± 6.3	21 ± 6.1	22 ± 6.8	.824[a]
Localization	14			
Central (*n*, %)	8	3 (42)	5 (55)	.592[b]
Limbs (*n*, %)	6	4 (57)	2 (22)	
Prior biopsy				
Yes (*n*, %)	3	-	3 (100)	.200[b]
No (*n*, %)	12	7 (58)	5 (42)	
Complete fractures (*n*, %)	7	4 (57)	3 (43)	.619[b]
Time of follow-up (mo)	25 (8-48)	26 (17-48)	24 (8-32)	.463[c]
Biochemical features at first visit				
Serum phosphate (mg/dL)	1.8 (0.8-3.6)	1.8 (1.4-3.6)	1.8 (0.8-2.5)	.613[c]
PTH (pg/mL)	73 (32-179)	73 (43-179)	67 (32-164)	.779[c]
ALP (IU/L)	297 (113-1839)	222 (113-355)	342 (130-1839)	.121[c]
β-CTX (ng/mL)	0.743 (0.096-2.126)	0.524 (0.425-1.255)	0.933 (0.096-2.126)	.189[c]
1,25OHD (ng/mL)	17 (6-48)	21 (6-40)	13 (7-48)	1.000[c]
iFGF23 (pg/mL)	138 (43-2253)	107 (54-179)	154 (43-2253)	.724[c]

Abbreviations: BMI, body mass index; PTH, parathyroid hormone; ALP, alkaline phosphatase; 1,25OHD, 1,25-hydroxyvitamin D; β-CTX, C-terminal cross-linked telopeptide of type I collagen; iFGF23 = fibroblast growth factor 23. [a]Student's *t*-test. [b]Fisher's exact test. [c]Mann–Whitney U test.

(Friedman test, $p = .908$). The median total hip BMD Z-score shifted from −2 (range: −5.7 to 1.3) at baseline to −1.1 (−4.3 to 0.8) at time point A, −0.7 (−4.3 to 1.8) at time point B, and 0.5 (−2.5 to 2.3) at time point C.

It is important to note that the negative values at the lower end of the ranges are attributed to two patients who had undergone long-term medical treatment prior to surgical cure. These patients (a 50-yr-old male and a 52-yr-old female) achieved normal BMD values before surgery. This insight can be better understood through the figures provided in Figure S1 and Figure S2.

Changes in bone microarchitecture

At the distal tibia, cortical area (Ct.Ar), cortical volumetric BMD (Ct.vBMD), and cortical thickness (Ct.Th) progressively increased from baseline to time point C (15%, $p = .04$; 3.4%, $p = .04$; and 14%, $p = .04$, respectively) (Table 2). Cortical porosity (Ct.Po) significantly increased by 27% at time point A compared to baseline ($p = .04$), stabilizing thereafter. Concurrently, trabecular parameters exhibited non-significant decreases with high dispersion. Stiffness and estimated failure load showed substantial, though non-significant, increases, peaking between baseline and time point A (14% and 13%, respectively) (Table 2). These structural changes are visually depicted in Figure 2, which illustrates HR-pQCT images of the distal tibia in a representative case from the resolved group—a 41-yr-old male with TIO who underwent curative surgery.

Cortical parameters at the distal radius remained stable throughout the follow-up, but with high dispersion of data (Table 3). At time point A, trabecular density and trabecular bone volume fraction (Tb.BV/TV) significantly decreased by 9.3% ($p = .01$) and 9.2% ($p = .01$), respectively.

Table 2. Median change in bone microarchitecture and bone strength parameters at distal tibia between baseline and time points A, B and C.

Tibia	Baseline to time A ($n=8$)	p^*	Baseline to time B ($n=12$)	p^*	Baseline to time C ($n=10$)	p^*	p^{**}
Geometry							
Tb.Ar, %	0.0 (−4.7 to 5.4)	-	−1.6 (−85.4 to 3.5)	-	−1.3 (−6.3 to 2.8)	-	.178
Ct.Ar, %	2 (−23.5 to 66.3)	1.000	8.4 (−19.2 to 181.3)	.518	15 (−13.3 to 254.9)	0.086	.041
Ct.Pm, %	0.2 (−0.4 to 1.8)	-	−0.1 (−1.8 to 0.8)	-	0.1 (−1.7 to 1.4)	-	.908
Volumetric density							
Tb.vBMD, %	−1.0 (−42.9 to 933.3)	-	−5.5 (−4500.0 to 1053.0)	-	2.0 (−60.9 to 1030.0)	-	.241
Ct.vBMD, %	−1.9 (−12.5 to 15.5)	-	0.3 (−8.3 to 24.9)	-	3.4 (−4.0 to 35.4)	-	.095
Microstructure							
Tb.N, %	−9.1 (−35.3 to 13.6)	-	−3.1 (−51.9 to 20.4)	-	−0.2 (−52.6 to 19.0)	-	.945
Tb.Th, %	−2.7 (−11.1 to 1550)	-	4.6 (−23.0 to 1725.0)	-	−6.7 (−200.0 to 1575.0)	-	.496
Tb.Sp, %	9.8 (−11.6 to 61.3)	-	3.3 (−16.3 to 118.3)	-	1.2 (−17.2 to 123.1)	-	.896
Tb.BV/TV, %	−1.3 (−42.5 to 1200)	-	−13.2 (−600 to 155.6)	-	−9.9 (−102.0 to 159.3)	-	.762
Ct.Th, %	2.3 (−23.7 to 65.7)	1.000	9 (−19.5 to 182.6)	.518	14 (−13.6 to 256.5)	0.086	.041
Ct.Po, %	26.7 (17.4 to 46.2)	-	−1.1 (−59.3 to 10.8)	-	1.7 (−1.8 to 5.3)	-	.127
FEA*							
Stiffness, %	13.8 (−4.4 to 11486.2)	-	12.1 (−23.9 to 69.7)	-	5.8 (−19.8 to 96.3)	-	.753
Failure load, %	12.8 (−3.0 to 54.7)	-	10.8 (−23.3 to 60.6)	-	5.3 (−19.4 to 89.7)	-	.753

Abbreviations: Tr.Ar, trabecular bone area; Ct.Ar, cortical bone area; Ct.Pm, cortical perimeter; Tb.vBMD, trabecular density; Ct.vBMD, cortical density; Tb.N, trabecular number; Tb.Th, trabecular thickness; Tb.Sp, trabecular separation; Ct.Th, cortical thickness; Tb.BVTV, trabecular bone volume fraction; Ct.Po, cortical porosity; FEA, finite element analysis. *Finite element analysis was available in 6 patients (4 from the resolved group and 2 from the non-resolved group). The values in parenthesis represent the range (minimum and maximum values). *Significance values have been adjusted by the Bonferroni correction for multiple tests. Multiple comparisons were not performed if the overall test is ≥0.05. **Related samples Friedman's two-way analysis of variance by ranks test.

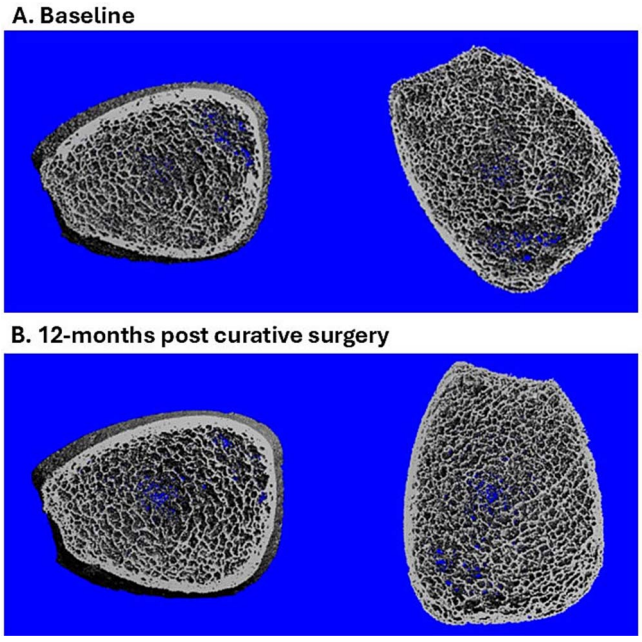

Figure 2. HR-pQCT images of the distal tibia in a representative case of a 41-yr-old male with tumor-induced osteomalacia, showing (A) baseline and (B) 12 mo post-curative surgery. At baseline, the cortical bone is difficult to distinguish, while post-surgery, it appears better defined.

Additionally, trabecular number (Tb.N) decreased by 9.1%, while trabecular separation (Tb.Sp) increased by 11.2%, both with borderline statistical significance ($p = .05$). At the final follow-up, trabecular parameters stabilized, going back to baseline. No significant changes were observed in stiffness or estimated failure load over time (Table 3).

To understand the relevance of these results, bone microarchitecture parameters from the ten patients with the longer-term follow-up were compared with a control group of 20 patients (Tables 4 and 5). At the distal tibia, long-term bone microarchitecture parameters in patients with TIO remained significantly lower compared with the control group, except for Ct.vBMD and Tb.Th. Specifically, Ct.vBMD showed a significant increase between baseline and long-term follow-up (+3.4%, $p = .049$), managing to approximate the control group (Table 4). At the radius, all parameters at time point C remained significantly lower compared to the control group, except for Ct.Th, whose values stayed lower compared to the control group but did not reach statistical significance (Table 5).

Differences in BMD, bone microarchitecture and bone strength between resolved and non-resolved groups

Median changes in lumbar spine BMD were higher in the resolved group compared to the non-resolved group, although these differences did not reach statistical significance (Figure 3). Specifically, median lumbar spine BMD changes were 21% vs 6% at time point A ($p = .905$), 44% vs 23% at time point B ($p = .366$), and 48% vs 10% at time point C ($p = .931$). Similarly, median changes in total hip BMD were greater in the resolved group, but the differences remained statistically non-significant. Median total hip BMD changes were 35% vs 0% at time point A ($p = .905$), 52% vs 9% at time point B ($p = .138$), and 72% vs 15% at time point C ($p = .247$).

In the resolved group, cortical porosity (Ct.Po) at the distal radius increased consistently, with statistically significant differences compared to the non-resolved group between baseline and time point A ($p = .04$) (Table S1). Specifically, changes in Ct.Po from baseline were 35% vs −17% at time point A, 34% vs 8.4% at time point B, and 21.5% vs −6.8% at time point C for the resolved and non-resolved groups, respectively. The remaining parameters did not show significant differences between the resolved and non-resolved groups (Table S1).

At the distal tibia, no significant differences were observed between the resolved and non-resolved groups. However, the data showed high variance (Table S2).

Table 3. Median change in bone microarchitecture and bone strength parameters at distal radius between baseline and time points A, B, and C.

Radio	Baseline to Time A ($n=8$)	p^*	Baseline to Time B ($n=12$)	p^*	Baseline to Time C ($n=10$)	p^{**}
Geometry						
Tb.Ar, %	1.4 (−1.4 to 4.5)	-	−0.2 (−4.8 to 5.2)	-	0.2 (−2.8 to 3.4)	.172
Ct.Ar, %	−7.1 (−99.9 to 139.6)	-	0.3 (−99.9 to 10.6)	-	0.6 (−99.9 to 10.3)	.532
Ct.Pm, %	0.0 (−0.5 to 1.1)	-	−0.1 (−2.5 to 0.7)	-	0.4 (−1.8 to 2.3)	.801
Volumetric density						
Tb.vBMD, %	−9.3 (−27.6 to −2.1)	-	0.7 (−12.9 to 32.9)	-	1.0 (−39.4 to 8.1)	.532
Ct.vBMD, %	−2.6 (−4.2 to 27.4)	-	0.5 (−5.0 to 3.4)	-	−0.5 (−3.4 to 5.5)	.072
Microstructure						
Tb.N, %	−9.1 (−39.3 to 9.4)	-	−4.2 (−26.0 to 15.3)	-	0.1 (−36.5 to 16.5)	.284
Tb.Th, %	−1.0 (−10.0 to 19.8)	-	2.2 (−18.5 to 42.3)	-	−2.2 (−20.0 to 17.6)	.167
Tb.Sp, %	11.2 (−8.0 to 71.9)	-	4.7 (−12.3 to 36.3)	-	0.9 (−13.3 to 68.2)	.284
Tb.BV/TV, %	−9.2 (−28.6 to -2.6)	-	0.8 (−12.5 to 60.0)	-	−0.1 (−99.0 to 30.0)	.532
Ct.Th, %	−7.5 (−16.9 to 166.7)	-	0.0 (−17.1 to 10.8)	-	−0.9 (−9.2 to 10.8)	.565
Ct.Po, %	0.7 (−61.4 to 42.9)	-	20.8 (−56.0 to 1220.2)	-	−2.1 (−61.3 to 89.0)	.615
FEA*						
Stiffness, %	−4.9 (−9.1 to 26.6)	-	6.6 (−13.5 to 8.9)	-	−0.2 (−19.6 to 73.1)	1.000
Failure load, %	−4.8 (−7.1 to 23.6)	-	7.9 (−11.4 to 12.6)	-	−0.5 (−18.4 to 65.9)	1.000

Abbreviations: Tr.Ar, trabecular bone area; Ct.Ar, cortical bone area; Ct.Pm, cortical perimeter; Tb.vBMD, trabecular density; Ct.vBMD, cortical density; Tb.N, trabecular number; Tb.Th, trabecular thickness; Tb.Sp, trabecular separation; Ct.Th, cortical thickness; Tb.BVTV, trabecular bone volume fraction; Ct.Po, cortical porosity; FEA, finite element analysis. *Finite element analysis was available in 6 patients (4 from the resolved group and 2 from the non-resolved group). The values in parentheses represent the range (minimum and maximum values). *Significance values have been adjusted by the Bonferroni correction for multiple tests. Multiple comparisons were not performed if the overall test is ≥0.05. **Related samples Friedman's two-way analysis of variance by ranks test.

Table 4. Median change in bone microarchitectural parameters between baseline and time point C at distal tibia in a subgroup of patients with long-term follow-up and comparison with a control group.

Tibia	Baseline	Time C	Median % increase between baseline and time C, p	Control group	Means difference	p^*
Tb.vBMD, mgHA/cm3	88.8 ± 57.6	88.0 ± 49.8	+2.0, .021	174.7 ± 50.5	−49.6	<.001
Ct.vBMD, mgHA/cm3	788.0 ± 120.3	840.1 ± 83.0	+3.4, .049	881.6 ± 54.2	−4.7	.110
Tb.N, 1/mm	1.12 ± 0.48	1.08 ± 0.56	−0.2, .586	1.98 ± 0.42	−45.4	<.001
Tb.Th, mm	0.060 ± 0.043	0.066 ± 0.032	−6.7, .524	0.074 ± 0.017	−10.8	.209
Tb.Sp, mm	1.072 ± 0.700	1.195 ± 0.791	+1.2, .261	0.454 ± 0.125	+163.2	<.001
Tb.BV/TV, %	6.5 ± 5.3	6.7 ± 5.0	−9.9, .752	14.5 ± 4.2	−53.8	<.001
Ct.Th, mm	0.71 ± 0.34	0.89 ± 0.26	+13.8, .040	1.22 ± 0.32	−27.0	.009

Abbreviations: Tb.vBMD, trabecular density; Ct.vBMD, cortical density; Tb.N, trabecular number; Tb.Th, trabecular thickness; Tb.Sp, trabecular separation; Ct.Th, cortical thickness; Tb.BVTV, trabecular bone volume fraction. *Comparison between time point C in patients with TIO (subgroup analysis of 10 patients with long-term follow-up) and control group.

Table 5. Median change in bone microarchitectural parameters between baseline and time point C at distal radius in a subgroup of patients with long-term follow-up and comparison with a control group.

Radius	Baseline	Time C	Median % increase between baseline and Time C, p	Control group	Diff means	p
Tb.vBMD, mgHA/cm3	137.0 ± 57.6	128.8 ± 53.3	0.6, 0.331	186.7 ± 53.6	−31.0	.009
Ct.vBMD, mgHA/cm3	832.2 ± 76.5	832.2 ± 72.9	−0.7, 0.997	876.5 ± 57.8	−5.0	.080
Tb.N, 1/mm	1.70 ± 0.43	1.66 ± 0.53	4.5, 0.687	2.02 ± 0.34	−17.8	.032
Tb.Th, mm	0.065 ± 0.014	0.063 ± 0.012	−3.2, 0.632	0.077 ± 0.015	−18.2	.016
Tb.Sp, mm	0.559 ± 0.183	0.601 ± 0.237	−4.2, 0.340	0.432 ± 0.087	−39.1	.008
Tb.BV/TV, %	9.8 ± 5.7	7.8 ± 5.5	−1.6, 0.330	15.6 ± 4.5	−50.0	<.001
Ct.Th, mm	0.68 ± 0.23	0.67 ± 0.22	−1.8, 0.318	0.81 ± 0.18	−17.3	.073

Abbreviations: Tb.vBMD, trabecular density; Ct.vBMD, cortical density; Tb.N, trabecular number; Tb.Th, trabecular thickness; Tb.Sp, trabecular separation; Ct.Th, cortical thickness; Tb.BVTV, trabecular bone volume fraction. *Comparison between time point C in patients with TIO (subgroup analysis of 10 patients with long-term follow-up) and control group.

Differences between patients with and without burosumab therapy

Changes in BMD and bone microarchitecture between baseline and time point C (long-term follow-up) were analyzed in the non-cured group, comparing patients treated with burosumab vs those receiving conventional therapy. Of the 6 evaluable patients, 4 were treated with burosumab, and 2 received conventional therapy. Due to the small sample size, comparisons at other time points were not feasible.

In patients receiving burosumab, lumbar spine BMD increased by a median of 27% (range: 10%-92%) compared to a median increase of 6% (range: 3%-8%) in those on

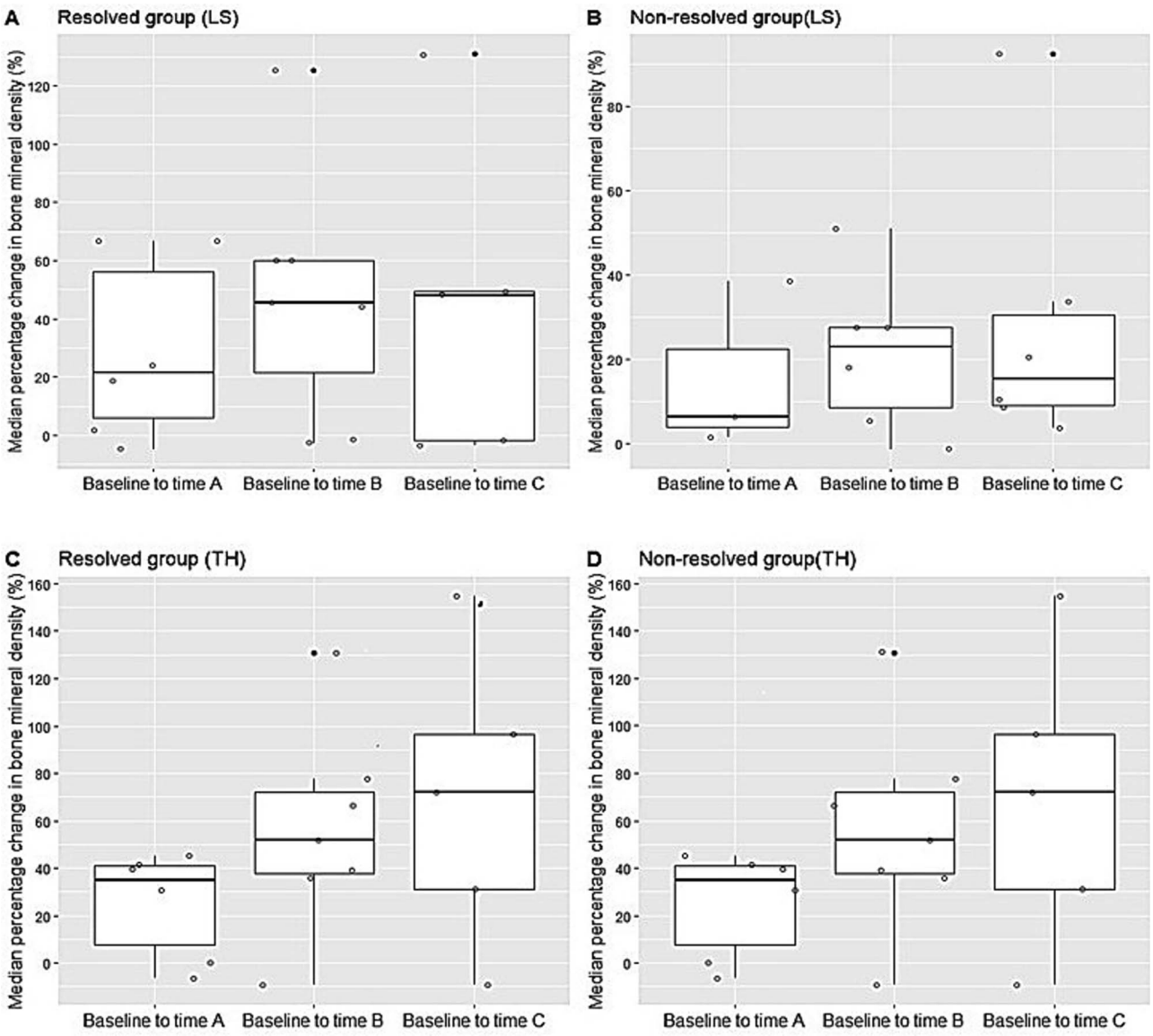

Figure 3. Median percentage changes in (A) lumbar spine and (B) total hip BMD between baseline and time points A, B, and C. Differences between resolved and non-resolved groups were not statistically significant at any time point.

conventional therapy (p = .133). Similarly, total hip BMD increased by a median of 31% (range: −33% to 44%) in the burosumab group vs a median increase of 9% (range: 9%-9%) in the conventional therapy group (p = .533). Changes in cortical parameters of bone microarchitecture were more pronounced in patients treated with burosumab; however, these differences did not reach statistical significance. For details, see Tables S3 and S4.

Correlations

We analyzed correlations between median changes in BMD, bone microarchitecture, bone strength, and bone turnover markers from baseline to time point C.

Increases in phosphate levels were associated with improvements in lumbar spine BMD ($\rho = 0.627$, p = .039). Greater decreases in ALP correlated with larger improvements in lumbar spine BMD ($\rho = -0.673$, p = .023), total hip BMD ($\rho = -0.855$, p = .001), Ct.Ar ($\rho = -0.636$, p = .048), Ct.Th ($\rho = -0.636$, p = .048) at the distal tibia, and Tb.BV/TV ($\rho = -0.661$, p = .038) at the distal radius. Additionally, changes in ALP were positively correlated with changes in Tb.Ar at the distal tibia ($\rho = 0.733$, p = .016).

Higher median changes in lumbar spine BMD were associated with greater changes in total hip BMD ($\rho = 0.809$, p = .003).

Finally, at the distal tibia, a larger increase in Ct.Ar was linked with higher Ct.vBMD ($\rho = 0.842$, p = .002), Tb.vBMD ($\rho = 0.648$, p = .043), and Ct.Th ($\rho = 1.000$, $p < .001$), and with a reduction in Tb.Ar ($\rho = -0.903$, $p < .001$). Cortical porosity (Ct.Po) was positively correlated with Tb.Ar ($\rho = 0.762$, p = .028) and negatively with Ct.Ar, Ct.vBMD, Ct.Th, and Tb.vBMD ($\rho = -0.714$, p = .047; $\rho = -0.762$, p = .028; $\rho = -0.714$, p = .047; $\rho = -0.786$, p = .021). A similar pattern was observed at distal radius (see Supplementary Material for details).

Discussion

This study provides a detailed analysis of long-term changes in BMD and bone microarchitecture in patients with TIO

following surgical cure or medical management. Our findings reveal significant improvements in BMD at lumbar spine and total hip, with the highest gains observed at a median time of 17 mo (range 12–21 mo), followed by continued but slower improvements until final follow-up. These results align with other studies that reported impressive gains of 29%-40% at the lumbar spine and 18%-38% at the total hip BMD during the early follow-up period (up to 3 mo).[4,5,10] In our study, these gains were sustained with a median follow-up of 26 mo. Remarkably, at the final follow-up, all patients achieved a normal lumbar spine BMD, while 91% attained a normal total hip BMD. Although we have not done bone biopsies, we hypothesized that primary mineralization after correction of the cause of the osteomalacia, is what explains the rapid changes of almost 30% observed in BMD. Additionally, significant and continuous long term changes might be due to the secondary mineralization of the previous osteoid bone.

BMD gains were accompanied by improvements in bone microarchitecture, particularly in cortical parameters, which translated into increased bone strength. Specifically, Ct.Th and Ct.vBMD showed progressive recovery, while Ct.Po stabilized after an initial increase. The significant improvements in cortical properties may reflect the ability of the skeleton to reconstitute lost cortical bone, which is crucial given the profound cortical deficits observed in patients with TIO.[5–7] The initial increase in distal tibia Ct.Po, along with stability or even decreases in Ct.thickness and Ct.v density, were similar to the findings by Ni et al.,[10] who observed similar patterns in patients recovering from TIO after 3 mo.[10] However, our study demonstrated that cortical parameters tended to improve over the long term.

Our results suggest a potential "mirror change" between cortical and trabecular bone areas throughout the recovery period. We hypothesize that during the active phase of TIO, endocortical bone undergoes ¨trabecularization¨ due to excessive phosphate loss and impaired mineralization, leading to a reduction in cortical thickness and area, while the trabecular area appears to increase. Following the resolution of TIO, this process may partially reverse as the endocortical compartment regains its "lost territory." The greater changes observed in cortical bone compared to trabecular bone could be explained by the larger surface area of cortical bone relative to the thin trabeculae, which may provide more potential for structural remodeling and mineral deposition.[13] This apparent worsening of trabecular parameters is also seen in the early changes in recovering patients in the study by Ni et al.[10] Additionally, a similar pattern of bone healing was reported in a 56-yr old woman from Brazil.[14] In this patient, at distal tibia, Tb.vBMD decreased whereas Ct.vBMD increased after 4 yr of tumor excision. On the contrary, microarchitectural parameters at distal radius were stable.[14] This hypothesis is further supported by the observed correlations observed in our study between changes in cortical and trabecular properties, highlighting the interconnected nature of these two bone compartments that take place in the endocortical area.

Improvements in cortical parameters of bone microarchitecture were more pronounced at the distal tibia than at the distal radius. A plausible explanation is that the tibia, as a weight-bearing bone, is more directly influenced by mechanical loading associated with ambulation. Many of these patients were previously limited in mobility and began walking as their condition improved with treatment/cure. This increased mechanical loading could stimulate bone remodeling processes in the tibia more rapidly compared to the radius.

The improvements in tibial bone microarchitecture translated into, although non-significantly, increased bone stiffness and estimated failure load, which are critical indicators of bone strength. As shown in previous research, bone strength is more significantly reduced when cortical microarchitecture is compromised compared to trabecular microarchitectural changes.[15] Notably, resolved patients in our cohort did not experience new fractures during the follow-up period, suggesting a clinically meaningful reduction in fracture risk as bone microarchitecture improved. This is a significant finding, given the high prevalence of fragility fractures in patients with active TIO.

Despite the positive trajectory of bone recovery, the final values of some microarchitectural parameters remained below those expected in healthy individuals, even when BMD returned to near-normal levels. However, tibial Ct.Thickness showed significant improvement and was not statistically different from the control group. This finding highlights the possibility that bone recovery may be incomplete in some patients, raising questions about the long-term structural integrity of bone in TIO survivors, especially in those with persistent deficits in bone microarchitecture despite achieving biochemical remission.

The differences between cured and non-cured patients were remarkable. Patients who achieved surgical cure showed more rapid and substantial improvements in both BMD and cortical microarchitecture, while non-cured patients exhibited slower and less pronounced changes. From a clinical perspective, this is particularly important, as patients receiving medical treatment may experience a longer recovery time, with more significant improvements becoming evident only after 17 mo.

Our exploratory analysis revealed potential differences in skeletal response between non-cured patients treated with burosumab vs conventional therapy. While not statistically significant due to the small sample size, trends suggested greater increases in BMD at both the lumbar spine and total hip in patients receiving burosumab compared to those on conventional therapy. Similarly, cortical bone microarchitecture improvements were more pronounced in the burosumab group, underscoring the potential of targeted therapy to enhance bone recovery in patients with TIO who do not achieve surgical cure.

The correlations observed between changes in BMD, bone microarchitecture, and laboratory parameters, such as serum phosphate and alkaline phosphatase (ALP) levels, provide insights into the mechanisms of bone recovery in TIO. Our previous study had demonstrated that ALP levels showed a negative correlation with microarchitecture parameters and bone strenght.[6] In histomorphometry analyses of patients with osteomalacia, higher serum ALP was associated with a lower mineral apposition rate and longer mineralization lag time,[16] suggesting that ALP may serve as a useful and inexpensive marker of bone quality in TIO patients.[17,18] Our results support the use of ALP monitoring as a valuable tool for assessing treatment response in TIO patients, potentially reflecting the extent of skeletal recovery.

Our study has several limitations. The small sample size limits the generalizability of our findings, and the clinical

heterogeneity of TIO patients—ranging from those achieving full biochemical remission to those with persistent physical disability from prior hip and/or vertebral fractures—adds complexity to the interpretation of results. This may partly explain the lack of statistical significance observed in the comparisons between resolved and non-resolved groups. Furthermore, while our study provides valuable long-term data, the variability in follow-up duration among patients may have influenced the observed trends. It is also important to acknowledge that, although HR-pQCT is a powerful in vivo imaging tool, it is insufficient to capture certain microstructural deficits and the cellular processes underlying bone formation, remodeling, and tissue-level mechanical properties. This limitation may lead to an underestimation of biological changes occurring during treatment. Additionally, the COVID-19 pandemic, which coincided with our study period, may have affected the consistency of follow-up visits and data collection, potentially introducing variability in patient monitoring and outcomes.

In conclusion, our study demonstrates that bone recovery in TIO is a prolonged process characterized by significant gains in BMD and microarchitectural improvements, particularly in cortical bone. While surgical cure is associated with a more pronounced recovery, medical therapy can also lead to meaningful skeletal improvements in non-cured patients. These findings underscore the importance of long-term monitoring and tailored therapeutic strategies to optimize bone health in patients with TIO.

Acknowledgments

We would like to thank Ego Seeman for his invaluable insights and contributions, which significantly enhanced the depth of our study.

Author contributions

María Belén Zanchetta collected and analyzed the data, designed the study, and revised the manuscript. Fernando Jerkovich analyzed and interpreted the data and drafted the manuscript. Florencia Scioscia, Yamile Mocarbel, Analía Pignatta, Natalia Elías, Juan Manuel Roganovich, Carlos Vigovich, María Celeste Balonga, Ana Carolina Cohen, Giselle Mumbach, José Luis Mansur, Carolina Fux Otta, Walter Guillermo Douthat, Pilar Tartaglia, Griselda Cecchi, María Bastianello, Luisa Plantalech, Erich Fradinger, and José Rubén Zanchetta collected the data. María Belén Zanchetta and Fernando Jerkovich are responsible for the integrity of the data analysis. All authors read and approved the final manuscript.

Supplementary material

Supplementary material is available at *JBMR Plus* online.

Funding

This study was partially funded by Ultragenyx as an Investigator Sponsored Trial (2020-2023) and by Fundación de Investigaciones Metabólicas (FIM). The funders of the study had no role in the study design, data collection, data interpretation or writing of the report. The authors had full access to all the data and had final responsibility for the decision to submit for publication.

Conflicts of interest

M.B.Z. is part of a Global TIO Disease Monitoring Program organized by Ultragenyx and serves as the chair of the DMP steering committee. M.C.B. has received honoraria from Ultragenyx as a speaker. The rest of the authors declare no potential conflicts of interest regarding this work.

Data availability

The datasets used and analyzed during the current study are available from the corresponding author upon reasonable request.

References

1. Minisola S, Peacock M, Fukumoto S, et al. Tumour-induced osteomalacia. *Nat Rev Dis Primers*. 2017;3(1):17044. https://doi.org/10.1038/nrdp.2017.44
2. Florenzano P, Hartley IR, Jimenez M, Roszko K, Gafni RI, Collins MT. Tumor-induced osteomalacia. *Calcif Tissue Int*. 2021;108(1):128-142. https://doi.org/10.1007/s00223-020-00691-6
3. Jerkovich F, Nuñez S, Mocarbel Y, et al. Burden of disease in patients with tumor-induced osteomalacia. *JBMR Plus*. 2020;5(2):e10436. https://doi.org/10.1002/jbm4.10436
4. Colangelo L, Pepe J, Nieddu L, et al. Long-term bone mineral density changes after surgical cure of patients with tumor-induced osteomalacia. *Osteoporos Int*. 2020;31(7):1383-1387. https://doi.org/10.1007/s00198-020-05369-1
5. Ni X, Feng Y, Guan W, et al. Bone impairment in a large cohort of Chinese patients with tumor-induced osteomalacia assessed by HR-pQCT and TBS. *J Bone Miner Res*. 2022;37(3):454-464. https://doi.org/10.1002/jbmr.4476
6. Zanchetta MB, Jerkovich F, Nuñez S, et al. Impaired bone microarchitecture and strength in patients with tumor-induced osteomalacia. *J Bone Miner Res*. 2021;36(8):1502-1509. https://doi.org/10.1002/jbmr.4325
7. Mendes DAB, Coelho MCA, Gehrke B, et al. Microarchitectural parameters and bone mineral density in patients with tumour-induced osteomalacia by HR-pQCT and DXA. *Clin Endocrinol*. 2021;95(4):587-594. https://doi.org/10.1111/cen.14533
8. Hacisahinogullari H, Tekin S, Tanrikulu S, et al. Diagnosis and management of tumor-induced osteomalacia: a single center experience. *Endocrine*. 2023;82(2):427-434. https://doi.org/10.1007/s12020-023-03450-3
9. Zhu Z, Xia W, Qi F, et al. Clinical characteristics and surgical outcomes of sinonasal lesions associated with tumor-induced osteomalacia. *Otolaryngol Head Neck Surg*. 2021;165(1):223-231. https://doi.org/10.1177/0194599820975432
10. Ni X, Zhang Z, Guan W, et al. Shift in calcium from peripheral bone to axial bone after tumor resection in patients with tumor-induced osteomalacia. *J Clin Endocrinol Metab*. 2023;108(11):e1365-e1373. https://doi.org/10.1210/clinem/dgad252
11. Silveira F, Monteverde C, Ripero V, Zanchetta MB, Massari F, Zanchetta JR. Reproducibility of HR-pQCT measurements in women with normal BMD and postmenopausal women with osteoporosis. *Osteoporos Int*. 2011;22(Suppl 1):S43-S44.
12. van Rietbergen B, Ito K. A survey of micro-finite element analysis for clinical assessment of bone strength: the first decade. *J Biomech*. 2015;48(5):832-841. https://doi.org/10.1016/j.jbiomech.2014.12.024
13. Seeman E. Age- and menopause-related bone loss compromise cortical and trabecular microstructure. *J Gerontol A Biol Sci Med Sci*. 2013;68(10):1218-1225. https://doi.org/10.1093/gerona/glt071
14. Salles, Rosa Neto N, RMR P, EFN Y, et al. Healing of tumor-induced osteomalacia as assessed by high-resolution peripheral quantitative computed tomography is not similar across the skeleton in the first years following complete tumor excision. *Bone Rep*. 2024;21:101758. https://doi.org/10.1016/j.bonr.2024.101758
15. Pistoia W, van Rietbergen B, Rüegsegger P. Mechanical consequences of different scenarios for simulated bone atrophy and

recovery in the distal radius. *Bone*. 2003;33(6):937-945. https://doi.org/10.1016/j.bone.2003.06.003
16. Bisballe S, Eriksen EF, Melsen F, Mosekilde L, Sørensen OH, Hessov I. Osteopenia and osteomalacia after gastrectomy: interrelations between biochemical markers of bone remodelling, vitamin D metabolites, and bone histomorphometry. *Gut*. 1991;32(11):1303-1307. https://doi.org/10.1136/gut.32.11.1303
17. Li F, Iqbal J, Wassif W, Kaddam I, Moniz C. Carboxyterminal propeptide of type I procollagen in osteomalacia. *Calcif Tissue Int*. 1994;55(2):90-93. https://doi.org/10.1007/BF00297181
18. Zanchetta MB, Corsi A. Bone biopsy for the diagnosis of osteomalacia. Can we avoid it? *J Bone Miner Res*. 2024;39(5):515-516. https://doi.org/10.1093/jbmr/zjae046

JBMR Plus, 2025, 9_ziaf041
https://doi.org/10.1093/jbmrpl/ziaf041
Research Article